Letter to the Editor

Imaging findings of sex cord tumor with annular tubules: a case description

Tingting Liu[1,2#], Xiaoqiong Li[1#], Yali Zhang[3], Weibin Dai[1], Donglian Du[1], Yueyou Peng[1], Kunkun Liu[1], Ningning Song[1], Tianfeng Shi[1], Yanfeng Meng[1,2]

[1]Department of Radiology, Taiyuan Central Hospital of Shanxi Medical University, Taiyuan, China; [2]Medical Imaging Department of Shanxi Medical University, Taiyuan, China; [3]Department of Pathology, Taiyuan Central Hospital of Shanxi Medical University, Taiyuan, China

[#]These authors contributed equally to this work.

Correspondence to: Yanfeng Meng, MD, PhD. Department of Radiology, Taiyuan Central Hospital of Shanxi Medical University, No. 1, East Sandao Lane, Jiefang Road, Xinghualing District, Taiyuan 030009, China. Email: yanfeng.m@163.com.

Submitted Dec 29, 2022. Accepted for publication May 19, 2023. Published online Jul 03, 2023.
doi: 10.21037/qims-22-1444
View this article at: https://dx.doi.org/10.21037/qims-22-1444

Introduction

Sex cord tumor with annular tubules (SCTAT) is an uncommon and distinctive type of ovarian sex cord-stromal tumor, accounting for fewer than 1% of all sex cord-stromal tumors (1,2). These tumors occur more in women of childbearing age and are often associated with Peutz-Jeghers syndrome (PJS) (3). To the best of our knowledge, only 1 case with imaging features of SCTAT and multilocular cystic mass was reported, and this was in 1995 (4). Here, we report a case with the imaging findings of a solid SCTAT without PJS.

Case presentation

A 66-year-old female visited Taiyuan Center Hospital of Shanxi Medical University complaining of recurrent postmenopausal vaginal bleeding for about 5 months. Natural pausimenia had occurred 8 years prior. Five months prior, she had discovered a small irregular vaginal brown hemorrhage with no obvious inducement that lasted for more than 10 days, but there was no abdominal pain or fever. After an interval of more than 10 days, vaginal bleeding occurred again. The hemorrhage was dark red and lasted for 4 months at which time she visited our clinic. Pelvic ultrasonography detected a hypoechoic mass in the left adnexal area with heterogeneous thickening of the endometrium (*Figure 1*). She was admitted to the hospital for further diagnosis and therapy. The patient was is poor spirits, but had a normal appetite, normal urine and stool, and no obvious weight loss.

In the physical examination, the unobstructed vagina appeared stained by dark red blood. The uterus was enlarged with normal mobility without tenderness. No obvious abnormality was found in the adnexal area, no abnormality was found in the genital organ or regarding any secondary sexual characteristics, and no pigmentation of the skin or mucosa was found. Laboratory test results were as follows: estradiol (E2) was 197.65 pg/mL, progesterone (P) was 1.38 ng/mL, and hemoglobin (HGB) was 86 g/L; meanwhile, serum carbohydrate antigen 125 (CA125), carbohydrate antigen 199 (CA199), and carcinoembryonic antigen (CEA) were normal (*Table 1*).

A plane computed tomography (CT) scan showed a mass of soft tissue in the left adnexal area, about 6.0 cm × 3.8 cm × 5.7 cm in size. CT attenuation values of the mass were inhomogeneous, and the range was 7–40 HU. The boundary of the mass was clear and tightly adjacent to the posterior wall of the uterus (*Figure 2*). Magnetic resonance imaging (MRI) showed a well-defined mass about 6.0 cm × 3.9 cm × 5.8 cm in size in the left adnexal area. The signal intensity (SI) of the mass was similar to that of the myometrium in T1-weighted imaging (T1WI) and slightly hyperintense in T2WI compared to that of the myometrium. There was a slightly lower SI in T1WI and higher SI in T2WI

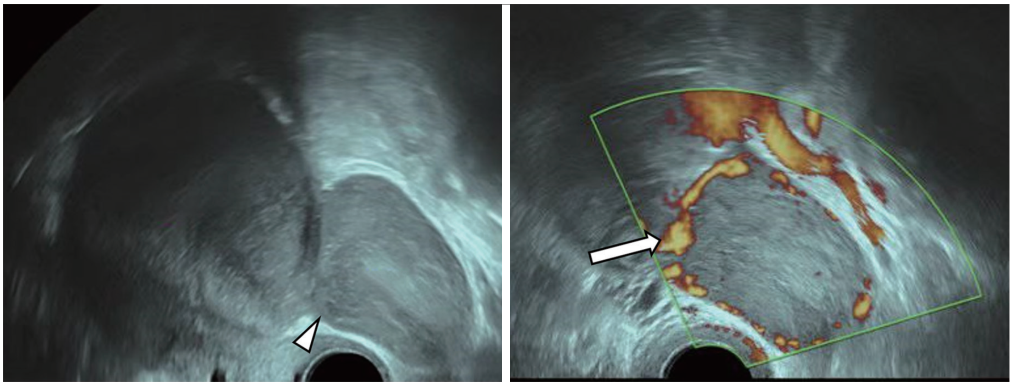

Figure 1 Pelvic ultrasonography detected a well-defined hypoechoic mass (white arrowhead) with blood flow signals (white arrow) visible in the left adnexal area.

Table 1 Summary of laboratory findings

Variables	Our patient's value	Reference range
WBC ($\times 10^9$/L)	6.16	3.5–9.5
RBC ($\times 10^{12}$/L)	3.74	3.7–5.1
PLT ($\times 10^9$/L)	179	125–350
HGB (g/L)	86	115–150
PRL (ng/mL)	22.41	3–21
FSH (mIU/mL)	0.18	14–76
LH (mIU/mL)	0.65	15.9–54
T (ng/dL)	76.98	14–76
E2 (pg/mL)	197.65	0–32.2
P (ng/mL)	1.38	0–0.73
CA125 (U/mL)	9.36	<34
CA199 (U/mL)	8.09	<35
CEA (ng/mL)	0.66	0–5
AFP (ng/mL)	1.16	0–10

WBC, white blood cell count; RBC, red blood cell count; PLT, platelet count; HGB, hemoglobin; PRL, prolactin; FSH, follicle-stimulating hormone; LH, luteinizing hormone; T, testosterone; E2, estradiol; P, progesterone; CA125, serum carbohydrate antigen 125; CA199, carbohydrate antigen 199; CEA, carcinoembryonic antigen; AFP, alpha fetoprotein.

in the areas of the mass. Diffusion-weighted imaging (DWI) showed diffusion restriction with hyperintensity with b value =800 s/mm^2, and the apparent diffusion coefficient (ADC) value was about 0.78×10^{-3} mm^2/s. There was no diffusion restriction found in the area of the mass with higher SI on T2WI. Gadolinium diamine (0.2 mL/kg) was injected through the elbow vein at a flow rate of 2 mL/s. The mass was progressively and inhomogeneously enhanced, and the enhancement degree in the delayed phase was significantly lower than that of the myometrium (*Figure 3*). There was no cervical mass or pelvic effusion found. Concerning the overall clinical impression, for the solid mass occupying the left adnexal area, ovarian sex cord-stromal tumor was considered.

In terms of surgery, hysteroscopy and segmental curettage were performed under intravenous anesthesia. Endometrial hyperplasia was diagnosed via pathology. Under laparoscopy, the mass, bilateral adnexa, and uterus were resected, and pelvic adhesiolysis was conducted under general anesthesia. The mass was solid, smooth on its surface, hard in texture, and grayish white in color. The patient recovered after this surgery without any related complications.

Pathological findings included a grayish red tissue about 7.5 cm × 5 cm × 5 cm in size that was smooth on its surface; gray, red, and light-yellow in color on the sectional view; and slightly brittle in gross appearance. Microscopically, the tumor cells were arrayed in circular tubules, and mild-red staining substances appeared in the lumen. The cells were oval, eosinophilic, and mild heteromorphic; cell nuclei were enlarged; and nuclear grooves were apparent. There were 4–5 mitotic figures per 10 high-power fields (*Figure 4*). The immunohistochemistry showed cytokeratin (CK; +), vimentin (+), Wilms' tumour-1 (WT-1, +), α-inhibin (+), calretinin (+), MelanA (partially weak +), CD99 (+), CD56 (+), progesterone receptors (PR; –), CK7 (–), epithelial membrane antigen (EMA; –), estrogen receptor (ER; –),

Figure 2 A CT scan showed a well-defined mass of soft tissue in the left adnexal area (white arrowhead). CT attenuation values of the mass were inhomogeneous, and the range was 7–40 HU. CT, computed tomography.

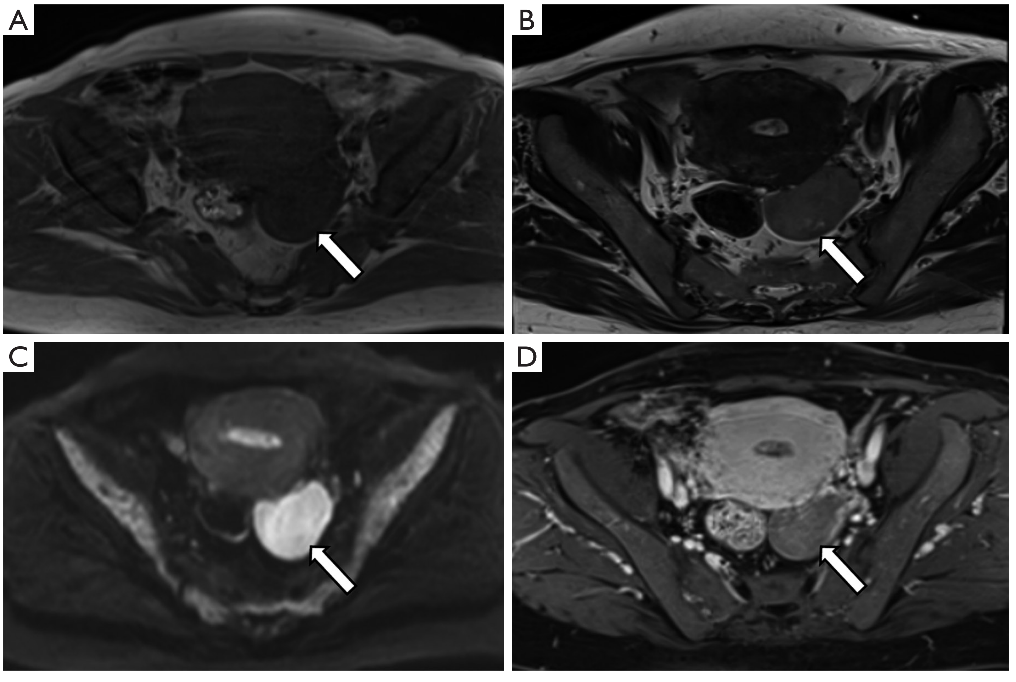

Figure 3 MRI scans showed a mass in the left adnexal area (white arrow). (A) The mass was isointense on T1WI as compared to the myometrium, containing slightly lower SI area and (B) slight hyperintensity in T2WI with higher SI areas in it. (C) DWI showed diffusion restriction. (D) The tumor was progressively and inhomogeneously enhanced, and the enhancement degree in the delayed phase was lower than that for the myometrium. MRI, magnetic resonance imaging; T1WI, T1-weighted imaging; SI, signal intensity; T2WI, T2-weighted imaging; DWI, diffusion-weighted imaging.

chromogranin A (CgA; –), CD10 (–), glypican-3 (GPC3; –), Sal-like protein 4 (SALL-4, –), and Ki-67 (+10%). The pathological diagnosis was SCTAT.

For follow-up, the patient underwent ultrasonography after being discharged from the hospital. No recurrence or metastasis has yet occurred.

All procedures performed in this study were in accordance with the ethical standards of the institutional committee of Taiyuan Central Hospital and with the Declaration of Helsinki (as revised in 2013). Written informed consent was obtained from the patient for publication of this case report and accompanying images. A copy of the written consent is available for review by the editorial office of this journal.

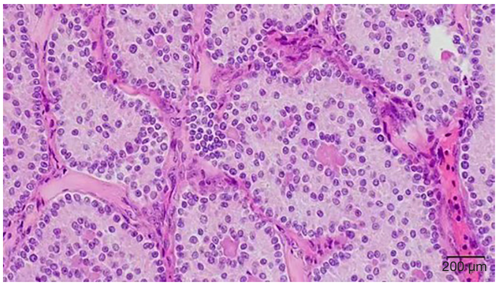

Figure 4 The tumor tissue was stained with hematoxylin and eosin. Staining revealed well-defined circular epithelial cells forming annular tubules of different sizes, cell nests, and a fibrous septum in the tumor. Scale bar: 200 μm.

Discussion

SCTAT is rare and a unique subtype of ovarian sex cord-stromal tumor. It often produces excessive estrogen and leads to premature puberty and irregular menstruation (5). The disease predominantly occurs in female patients aged 30–40 years old, but studies have reported that the disease can occur in a wider age range (4–74 years old) (6,7). The tumor is characterized by well-defined circular epithelial cell nests, forming annular tubules surrounding eosinophilic transparent bodies. There are two different patterns of nests. One pattern includes closed tubules and a central transparent body. The other pattern includes continuous tubular nests revolving around multiple transparent bodies (1). Immunohistochemical markers are characterized by the positive expression of inhibin-A, calretinin, WT-1, CK, and vimentin, and the negative expression of cellular tumor antigen p53 (P53), alpha-fetoprotein (AFP), EMA, placental alkaline phosphatase (PLAP), laminin, and CD117 (3). The pathological morphology of SCTAT lies between that of giant cell tumor (GCT) and Sertoli cell tumor (SCT), and it may locally differentiate into either of them (8). In clinic, about one-third of SCTAT cases are related to PJS, which generally shows bilateral, small, and calcified benign tumors. However, about 20% of patients with SCTAT are not accompanied by PJS, and these patients appear with usually unilateral, single, and large malignant tumors (9,10). Most patients with SCTAT have elevated estrogen levels, menstrual disorders, precocious puberty, infertility, amenorrhea, and postmenopausal vaginal bleeding (1,2,11).

Thus far, only 1 case report has been published that includes the imaging features of SCTAT. According to limited information from clinical reports, SCTAT can a be cystic, cystic-solid, or solid mass. In the case presented in this report, the imaging feature of SCTAT was obviously different from that of other ovarian sex cord-stromal tumors, such as fibrothecoma, GCT, and SCT. Fibrothecoma is the most common tumor among all ovarian sex cord-stromal tumors, and it is solid or mainly solid. The imaging feature depends on the ratio of fibers to theca cells. MRI can distinguish different components. Although it is mainly composed of fibers, the tumor shows a significantly low SI on T2WI in the solid areas. With a decrease in the number of fibers and the increase in the number of theca cells, T2WI SI gradually increases from iso-low to slightly high SI. Although the tumor is mainly composed of theca cells, which contain rich lipids, dual-echo chemical-shift MRI can identify lipids contained in the tumor (12,13). GCT has different gross pathological features according to different tissue types, which can be mainly solid to unilocular cystic or multilocular cystic (14). A typical feature is solid tumors with different cystic changes and intratumoral hemorrhage (15). Therefore, hyperintensity is often encountered in T1WI of GCT, which can be used to distinguish SCTAT. In addition, studies have also reported non-bleeding GCT, which can appear as lobulated solid masses with cysts or in a pure solid mass. A lobulated solid mass with cysts can be differentiated from SCTAT according to its lobulated profile. Pure solid masses can be accompanied by a decreased uterine volume and endometrial atrophy, as well as clinical manifestations of amenorrhea (14,16). SCTs are also usually solid or mainly solid. The solid part of the tumor shows significant enhancement when a contrast agent is used, which is quite different from what occurred in this case (17).

In the past, only 1 case of a 7-year-old girl with elevated estradiol and without vaginal bleeding was reported with imaging features; she had a multilocular cystic mass with a thin septa and homogeneous thickness. On enhanced scans, the cyst wall and septa were slightly enhanced. Pathological results confirmed SCTAT after left salpingo-oophorectomy (4). In this case, the patient was an older adult woman with irregular vaginal bleeding. The mass was solid, T2WI showed slight hyperintensity, diffusion of the tumor was restricted, and dynamic enhanced scanning showed progressive and inhomogeneous enhancement. The imaging feature of this tumor was a consistently solid mass with a clear boundary on ultrasonography, CT, and MRI. MRI has advantages in the evaluation of SCTAT by virtue of its excellent tissue contrast, multiparameter imaging ability, and sensitivity to lesion enhancement, and thus it provides more detailed information as compared to ultrasonography or CT.

A few limitations to this report should be discussed. Thus far, only a single report of the imaging features of SCTAT has been published, the details of which differ from those of this case. It is thus difficult to draw a conclusion concerning the imaging features of SCTAT. However, this case provides new information for the radiological diagnosis of SCTAT which may inform the preoperative differential diagnosis of SCTAT in older adult women.

Acknowledgments

Funding: None.

Footnote

Conflicts of Interest: All authors have completed the ICMJE uniform disclosure form (available at https://qims.amegroups.com/article/view/10.21037/qims-22-1444/coif). The authors have no conflicts of interest to declare.

Ethical Statement: The authors are accountable for all aspects of the work in ensuring that questions related to the accuracy or integrity of any part of the work are appropriately investigated and resolved. All procedures performed in this study were in accordance with the ethical standards of the institutional committee of Taiyuan Central Hospital and with the Helsinki Declaration (as revised in 2013). Written informed consent was obtained from the patient for publication of this case report and accompanying images. A copy of the written consent is available for review by the editorial office of this journal.

References

1. Scully RE. Sex cord tumor with annular tubules a distinctive ovarian tumor of the Peutz-Jeghers syndrome. Cancer 1970;25:1107-21.
2. Qian Q, You Y, Yang J, Cao D, Zhu Z, Wu M, Chen J, Lang J, Shen K. Management and prognosis of patients with ovarian sex cord tumor with annular tubules: a retrospective study. BMC Cancer 2015;15:270.
3. Yahaya JJ, Mshana D, Mremi A. Ovarian sex cord tumour with annular tubules in a 13-year-old female: a case report. Oxf Med Case Reports 2020;2020:omaa024.
4. Moon WK, Kim SH, Kim WS, Kim IO, Yeon KM, Han MC. Case report: ovarian sex cord tumour with annular tubules: imaging findings. Clin Radiol 1995;50:581-2.
5. Ishikawa H, Kiyokawa T, Takatani T, Wen WG, Shozu M. Giant multilocular sex cord tumor with annular tubules associated with precocious puberty. Am J Obstet Gynecol 2012;206:e14-6.
6. Chen X, Crapanzano JP, Gonzalez AA, Hamele-Bena D. Cytologic features of needle aspiration of ovarian sex cord tumor with annular tubules: Report of two cases and literature review. Diagn Cytopathol 2018;46:627-31.
7. Chang RJ, Reuther J, Gandhi I, Roy A, Jain S, Masand RP. Sex Cord Tumor With Annular Tubules-Like Histologic Pattern in Adult Granulosa Cell Tumor: Case Report of a Hitherto Unreported Morphologic Variant. Int J Surg Pathol 2021;29:433-7.
8. Young RH, Welch WR, Dickersin GR, Scully RE. Ovarian sex cord tumor with annular tubules: review of 74 cases including 27 with Peutz-Jeghers syndrome and four with adenoma malignum of the cervix. Cancer 1982;50:1384-402.
9. Chatziioannidou K, Botsikas D, Tille JC, Dubuisson J. Preservation of fertility in non-Peutz-Jegher syndrome-associated ovarian sex cord tumour with annular tubules. BMJ Case Rep 2015.
10. Senn D, Videira H, Haagsma B, El-Bahrawy M, Madhuri TK. Sex Cord Tumour with Annular Tubules-An Unusual Case of Abdominal Pain. J Obstet Gynaecol Can 2021;43:361-4.
11. Lele SM, Sawh RN, Zaharopoulos P, Adesokan A, Smith M, Linhart JM, Arrastia CD, Krigman HR. Malignant ovarian sex cord tumor with annular tubules in a patient with Peutz-Jeghers syndrome: a case report. Mod Pathol 2000;13:466-70.
12. Okajima Y, Matsuo Y, Tamura A, Irie H, Nakazono T, Hara Y, Suzuki K, Yamasaki F, Kudo S, Saida Y. Intracellular lipid in ovarian thecomas detected by dual-echo chemical shift magnetic resonance imaging: report of 2 cases. J Comput Assist Tomogr 2010;34:223-5.
13. Jung SE, Lee JM, Rha SE, Byun JY, Jung JI, Hahn ST.

CT and MR imaging of ovarian tumors with emphasis on differential diagnosis. Radiographics 2002;22:1305-25.
14. Ko SF, Wan YL, Ng SH, Lee TY, Lin JW, Chen WJ, Kung FT, Tsai CC. Adult ovarian granulosa cell tumors: spectrum of sonographic and CT findings with pathologic correlation. AJR Am J Roentgenol 1999;172:1227-33.
15. Tanaka YO, Tsunoda H, Kitagawa Y, Ueno T, Yoshikawa H, Saida Y. Functioning ovarian tumors: direct and indirect findings at MR imaging. Radiographics 2004;24 Suppl 1:S147-66.
16. Kim SH, Kim SH. Granulosa cell tumor of the ovary: common findings and unusual appearances on CT and MR. J Comput Assist Tomogr 2002;26:756-61.
17. Wang PH, Chao HT, Lee RC, Lai CR, Lee WL, Kwok CF, Yuan CC, Ng HT. Steroid cell tumors of the ovary: clinical, ultrasonic, and MRI diagnosis--a case report. Eur J Radiol 1998;26:269-73.

Cite this article as: Liu T, Li X, Zhang Y, Dai W, Du D, Peng Y, Liu K, Song N, Shi T, Meng Y. Imaging findings of sex cord tumor with annular tubules: a case description. Quant Imaging Med Surg 2023;13(8):5403-5408. doi: 10.21037/qims-22-1444